NEW TYPE OF NEGATIVE RESISTANCE IN BARRIER TUNNELING

L. Esaki and P. J. Stiles
IBM Watson Research Center, Yorktown Heights, New York
(Received 20 April 1966)

It is shown theoretically that, under certain conditions, the current-voltage characteristic of an insulating barrier tunnel junction between a metal and a degenerate semiconductor exhibits a negative resistance, similar to that of the tunnel diode.[1] This new type of negative resistance arises from the voltage dependence of the tunneling probability of the barrier. We have recently observed this negative resistance in the tunnel junction of Al-Al_2O_3-SnTe system in the course of studying the electronic band structure of SnTe by tunneling spectroscopy. Another significance in the present tunnel-junction characteristic is that this is the first observation of the "thermal" energy gap in SnTe.

Energy diagrams in Fig. 1 schematically illustrate four types of tunnel junctions with a thin insulating layer of thickness d at zero bias voltage. It can be assumed that, in the wave-number space, a relatively small shadow cast on a barrier plane by a constant-energy surface for electrons in the conduction or valence band of the semiconductor is always covered with a large shadow cast by that of the metal. This implies, assuming the conservation of the transverse wave number k_t, that tunneling electrons from the semiconductor have no difficulty finding a site available in the metal.

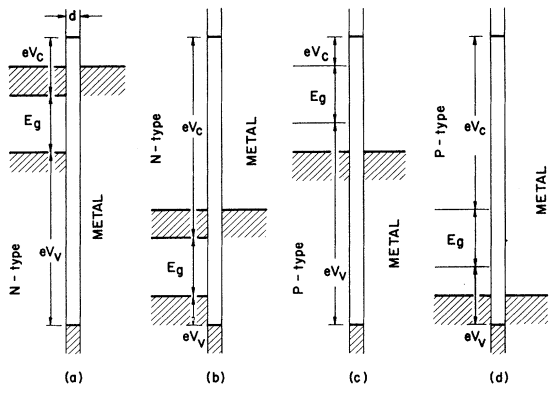

FIG. 1. Schematic illustration of four junctions of electron tunneling between a metal and a degenerate semiconductor with the energy gap E_g through a thin insulating layer at zero bias voltage. The hatched region indicates filled states. (a) n type with $V_C < V_v$, no negative resistance, (b) n type with $V_v < V_C$, negative resistance; (c) p type with $V_C < V_v$, negative resistance; and (d) p type with $V_v < V_C$, no negative resistance.

Now, using the WKB approximation,[2] the tunneling current I at zero temperature is simply given by the following double integral with the well-known tunneling exponent λ:

$$I = A\int\int \exp(-\lambda) dE_t dE, \quad -\lambda = -2\int |k_x| dx, \qquad (1)$$

where E and E_t are the total and transverse kinetic energies of electrons in the semiconductor, respectively, and k_x is the imaginary wave number normal to the junction plane inside the forbidden gap in the insulating layer. In Fig. 1, E_g is the energy gap of the semiconductor, and eV_C and eV_v are the energy differences of the conduction-band bottom and the valence-band top between the semiconductor and the insulator, respectively. The slope of the band edges in the insulator is, of course, dependent upon the applied voltage V. No slope is assumed at zero bias voltage. Here we are neglecting image forces, band bending near the interface, and surface states, as well as any tail states near the band edge.[3]

Now let us estimate the tunneling exponent λ_C for the conduction band and λ_v for the valence band in the four cases in Fig. 1. The exponents corresponding to Figs. 1(a), 1(b), 1(c), and 1(d) are identified as λ_C(I), λ_C(II), λ_v(I), and λ_v(II), respectively. We approximate further by assuming that k_x at given E and E_t is determined only by the smaller of the energy differences between the electron energy in the semiconductor and the conduction- and valence-band edges in the insulator.

With all approximations mentioned above, we have

$$\lambda_C(I) = \frac{2(2|m_i|)^{1/2}}{\hbar}\int_0^d \left(eV_C - E + \frac{m_s}{m_i}E_t - \frac{eVx}{d}\right)^{1/2} dx,$$

$$\lambda_C(II) = \frac{2(2|m_i|)^{1/2}}{\hbar}\int_0^d \left(eV_v' + E - \frac{m_s}{m_i}E_t + \frac{eVx}{d}\right)^{1/2} dx,$$

$$\lambda_v(I) = \frac{2(2|m_i|)^{1/2}}{\hbar}\int_0^d \left(eV_c' + E - \frac{m_s}{m_i}E_t + \frac{eVx}{d}\right)^{1/2} dx,$$

$$\lambda_v(II) = \frac{2(2|m_i|)^{1/2}}{\hbar}\int_0^d \left(eV_v - E + \frac{m_s}{m_i}E_t - \frac{eVx}{d}\right)^{1/2} dx,$$

where $V_C' = V_C + E_g/e$ and $V_v' = V_v + E_g/e$, and m_i and m_s are the effective masses in the insulator and the semiconductor, respectively, assuming the spherical band structure. The applied voltage V is assumed to be positive in the cases of λ_C(I) and λ_C(II) if the metal side is positively biased with respect to the semiconductor, and in the cases of λ_v(I) and λ_v(II) if the semiconductor side is positively biased with respect to the metal. With this voltage convention, a structure due to the energy gap can be seen only under positively applied voltage, and with increase in positive voltage, λ_C(II) and λ_v(I) increase, namely, the tunneling probability decreases, whereas λ_C(I) and λ_v(II) decrease. It is also interesting to note that, in the cases λ_C(II) and λ_v(I), low-energy electrons of small E have a larger tunneling probability than high-energy electrons, and that the effective mass must flip its sign when the electron crosses the boundary between the semiconductor and the insulator, because of the opposite curvature in the E-k relationship.[4]

We first examine the theoretical current-voltage characteristic in these cases, namely, the n-type case with $V_v < V_C$ in Fig. 1(b) and the p-type case with $V_C < V_v$ in Fig. 1(c). We will treat only the p-type case, as the n-type case has exactly the same form. The currents I_C and I_v due to the conduction band and the valence band, respectively, easily derived as a function of applied voltage from Eq. (1) and the expressions for the λ's, are approximately as follows, assuming that the absolute value of the effective mass is the same in all regions: For $eV < F_p$,

$$I_v = [A/(\alpha'\beta')^2]\exp(-\alpha')\exp(-\tfrac{1}{2}\alpha'\beta' eV) \times \exp(-\alpha'\beta' F_p)\{\exp(\alpha'\beta' eV) - 1 - \tfrac{1}{2}\exp[\alpha'\beta'(2eV - F_p)] + \tfrac{1}{2}\exp(-\alpha'\beta' F_p)\}, \quad (2)$$

where F_p is the Fermi energy of the semiconductor. For $F_p < eV$,

$$I_v = [A/(\alpha'\beta')^2]\exp(-\alpha')\exp(-\tfrac{1}{2}\alpha'\beta' eV) \times [\tfrac{1}{2} - \exp(-\alpha'\beta' F_p) + \tfrac{1}{2}\exp(-2\alpha'\beta' F_p)]. \quad (3)$$

For $F_p + E_g < eV$, the following current I_C will be introduced in addition to the above current I_v:

$$I_C = [A/(\alpha\beta)^2]\exp(-\alpha)\exp(-\tfrac{1}{2}\alpha\beta eV) \times \{\exp[\alpha\beta(eV - F_p - E_g)] - 1 - \alpha\beta(eV - F_p - E_g)\}, \quad (4)$$

where

$$\alpha = (2d/\hbar)(2|m_i|eV_C)^{1/2}, \quad \beta = 1/2eV_C,$$

and α' and β' are given by substituting V_C' for V_C.

The current I_v is particularly interesting because it shows a maximum around $eV = F_p$ and then decreases with further increase in V, namely, it illustrates a negative-resistance region. On the other hand, the current I_C starts at $eV = F_p + E_g$ and soon offsets this I_v negative resistance with further increase in V. The conductance is simply obtained by differentiating Eqs. (2), (3), and (4).[5]

Now, in the same way, one can derive the current I_C and I_v in the p-type case with $V_v < V_C$ in Fig. 1(d)[6] as well as in the n-type case with $V_C < V_v$ in Fig. 1(a). Some minor structure corresponding to the energy gap is expected without any negative resistance in these cases.

Figures 2(a) and 2(b) show current-voltage curves at 4.2, 77, and 300°K, and, with a solid line, a conductance plot at 4.2°K experimentally observed in the tunnel junction of Al-Al_2O_3-SnTe, which was made by evaporating SnTe onto an oxidized evaporated stripe of Al. The negative resistance is seen between 0.55 and 0.85 V. The SnTe layer is highly p type with about 8×10^{20} carriers/cm^3. The barrier height of Al_2O_3 was estimated to be 1.5-2 eV,[7] while its energy gap is probably as high as 8 eV.[8] Therefore, we could well apply the case of Fig. 1(c) to this junction. In Fig. 2(b), a calculated conductance plot[5] is shown with a dashed line, assuming 2-eV barrier height, $\alpha = 20$, $F_p = 0.6$ eV, and $E_g = 0.3$ eV.

The shapes of the theoretical and experimental curves[9] are sufficiently alike so that the present result seems to establish that our evaporated polycrystalline SnTe is definitely a semiconductor.[10] The experimental result indicates that the thermal energy gap E_g is 0.30 ± 0.05 eV at 4.2°K, and the Fermi energy F_p is 0.60 $\pm$ 0.05 eV, giving the average density-of-state mass in the valence band to be about half of

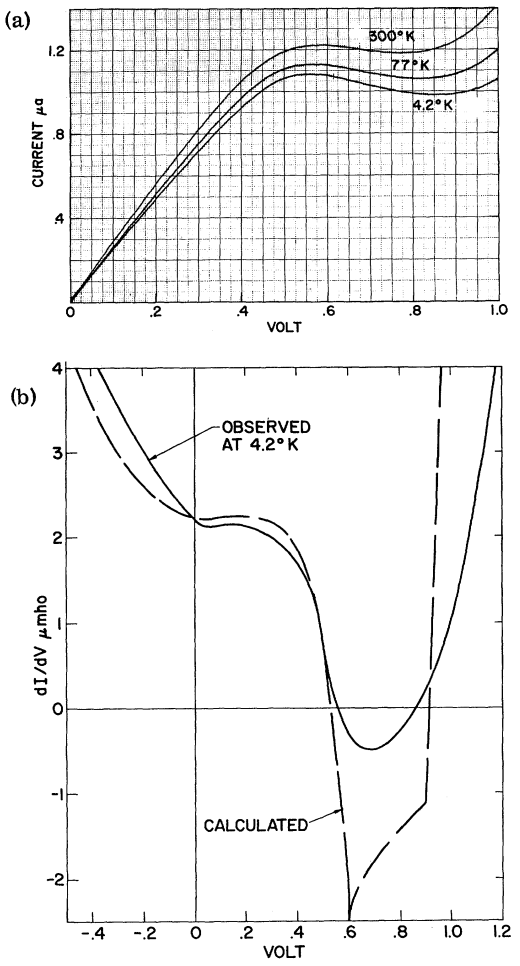

FIG. 2. (a) Experimental current-voltage curves at 4.2, 77, and 300°K in the tunnel junction of Al-Al_2O_3-SnTe. (b) Observed conductance at 4.2°K (solid line) and calculated one (dashed line), assuming 2-eV barrier height, $\alpha = 20$, $F_p = 0.6$ eV, and $E_g = 0.3$ eV, and zero temperature. The calculated conductance is scaled so that the value at zero bias voltage coincides with that observed.

the free-electron mass.

The combination of evaporated SnTe and oxidized Al barrier has turned out to be quite suitable for obtaining this type of negative resistance, which not only plays a salient role in tunneling spectroscopy[11] but also bears a potential in practical use. There must be other combinations of semiconductors and insulating barriers satisfying the above-described conditions and thus showing negative resistance. That remains to be explored.

We wish to thank W. E. Howard who is involved in the experimental program on the band structure of SnTe. It is also a pleasure to acknowledge helpful discussions with R. R. Haering, L. L. Chang, and N. Wiser on the voltage dependence of the tunneling probability.

[1]L. Esaki, Phys. Rev. 109, 603 (1958).

[2]W. A. Harrison, Phys. Rev. 123, 85 (1961).

[3]All these effects would contribute toward smearing the characteristic of our tunnel junctions.

[4]We owe this consideration to T. N. Morgan.

[5]For $eV < F_p$

$$\frac{dI_v}{dV} = \frac{eA}{2(\alpha'\beta')}\exp(-\alpha')\exp(-\tfrac{1}{2}\alpha'\beta' eV)\exp(-\alpha'\beta' F_p)$$
$$\times\{\exp(\alpha'\beta' eV) + 1 - \tfrac{3}{2}\exp[\alpha'\beta'(2eV - F_p)] - \tfrac{1}{2}\exp(-\alpha'\beta' F_p)\};$$

for $F_p < eV$,

$$\frac{dI_v}{dV} = \frac{eA}{2(\alpha'\beta')}\exp(-\alpha')\exp(-\tfrac{1}{2}\alpha'\beta' eV) \times[\exp(-\alpha'\beta' F_p) - \tfrac{1}{2} - \tfrac{1}{2}\exp(-2\alpha'\beta' F_p)];$$

and for $F_p + E_g < eV$,

$$\frac{dI_c}{dV} = \frac{eA}{2(\alpha\beta)}\exp(-\alpha)\exp(-\tfrac{1}{2}\alpha\beta eV) \times\{\exp[\alpha\beta(eV - F_p - E_g)] - 1 + \alpha\beta(eV - F_p - E_g)\}.$$

[6]For $eV < F_p$,

$$I_v = \frac{A}{(\alpha\beta)^2}\exp(-\alpha)\exp(\tfrac{1}{2}\alpha\beta eV) \times\{\exp(\alpha\beta F_p) - \exp[\alpha\beta(F_p - eV)] - \alpha\beta eV\};$$

for $F_p < eV$,

$$I_v = [A/(\alpha\beta)^2]\exp(-\alpha)\exp(\tfrac{1}{2}\alpha\beta eV)[\exp(\alpha\beta F_p) - 1 - \alpha\beta F_p];$$

and for $F_p + E_g < eV$, I_c is introduced in addition to I_v,

$$I_c = [A/(\alpha\beta)^2]\exp(-\alpha')\exp(\tfrac{1}{2}\alpha'\beta' eV) \times\{\tfrac{1}{2} - \exp[-\alpha'\beta'(eV - F_p - E_g)] + \tfrac{1}{2}\exp[-2\alpha'\beta'(eV - F_p - E_g)]\},$$

where

$$\alpha = (2d/\hbar)(2|m_i|eV_v)^{1/2}, \quad \beta = 1/2eV_v,$$

and α' and β' are given by substituting V_v' for V_v.

[7]S. R. Pollack and C. E. Morris, Trans. AIME 233, 497 (1965); O. L. Nelson and D. E. Anderson, J. Appl. Phys. 37, 77 (1966).

[8]See, for instance, American Institute of Physics Handbook (McGraw-Hill Book Company, Inc., New York, 1963), 2nd ed., p. 6-66, Fig. 6c-24.

[9]N. Wiser has carried out the calculation of the con-

ductance with the sharp boundary condition,[2] namely, exact matching of the wave functions, rather than with the WKB approximation. His result eliminates the cusp at $eV = F_p$ and thus is closer to the experimental result. However, quantitative discrepancy between the theory and the experiment in the negative-resistance region is believed to be due to the simplification employed here. See Ref. 3.

[10]J. A. Kafalas, R. F. Brebrick, and A. J. Strauss, Appl. Phys. Letters 4, 93 (1964); B. G. Bylander, J. R. Dixon, H. R. Riedl, and R. B. Schoolar, Phys. Rev. 138, A864 (1965); B. A. Efimova, V. I. Kaidanov, B. Ya. Moizhes, and I. A. Chernik, Fiz. Tverd. Tela 7, 2524 (1965) [translation: Soviet Phys.—Solid State 7, 2032 (1966)].

[11]The present effect would not be important as long as the applied voltage is kept low in comparison with the barrier height as seen in L. Esaki and P. J. Stiles, Phys. Rev. Letters 14, 902 (1965); 16, 574 (1966). In such cases, one can assume the tunneling exponent λ to be virtually constant in Eq. (1), as was done in Ref. 2.

SPIN-CLUSTER RESONANCE IN $CoCl_2 \cdot 2H_2O$

Muneyuki Date and Mitsuhiro Motokawa
Department of Physics, Faculty of Science, Osaka University, Toyonaka, Osaka, Japan
(Received 2 May 1966)

A new type of magnetic resonance has been observed in $CoCl_2 \cdot 2H_2O$ at low temperatures. This compound is antiferromagnetic below 17.2°K with an antiferromagnetic arrangement of ferromagnetic linear chains. Exchange interactions among chains are antiferromagnetic while a strong ferromagnetic exchange interaction exists in the chain and an anisotropy favoring the b axis is so strong that the spin system can be looked at nearly as a bundle of Ising spin chains.[1,2] When an external magnetic field is applied along the b axis, the magnetization increases stepwise with increasing field[3,4] and, as was preliminarily reported by the present authors, curious resonances are observed[5] near the critical fields H_{c1} and H_{c2} (see Fig. 1). These resonances, which have been excited with microwaves of 24-70 Gc/sec in a pulsed magnetic field up to 50 kOe, are very different from usual ferromagnetic or antiferromagnetic resonances. For instance, the absorption intensity is weak and decreases rapidly with decreasing temperature from 4.2 to 1.5°K. We have now been able to analyze the detailed structure of the resonances and find that these absorptions come from a spin-cluster resonance with the selection rule $\Delta m = \pm 1$, where m is the number of spins in a short-range-order spin cluster directed opposite to the majority spins in a ferromagnetic chain.

Let us consider an Ising spin chain coupled by a ferromagnetic exchange interaction J_0, with an external magnetic field H_0 parallel to the spin easy axis (the b axis in $CoCl_2 \cdot 2H_2O$) which we take as the z axis. There is no phase transition in such a system, but almost all spins point along H_0 for a sufficiently strong field at low temperatures. However, some spins point toward $-z$ so as to minimize the free energy. Examples of spin clusters are shown in Fig. 2(a). Neglecting dipolar interactions, the resonance condition for the allowed transitions $\Delta m = \pm 1$ is simply $\omega/\gamma = H_0$. It should be emphasized that the resonance frequency for a spin-cluster transition does not depend on J_0 as there is no change in exchange ener-

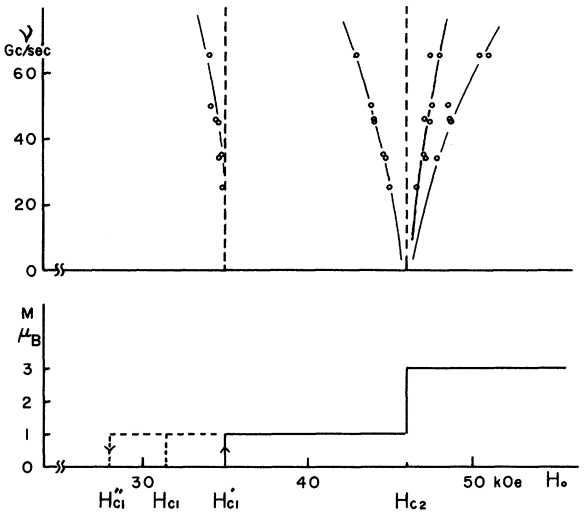

FIG. 1. Frequency-field diagram of the resonance points and corresponding changes of the magnetization ($H_0 \parallel b$ axis). H_{c1} is the thermodynamic critical field for the lower transition, but because of hysteresis, this transition is observed at H_{c1}' on increasing the field, and at H_{c2}'' when the field is decreased. Resonances near the lower transition field can only be observed in an increasing magnetic field, near H_{c1}'.